Journal of Zhejiang University SCIENCE A
ISSN 1673-565X (Print); ISSN 1862-1775 (Online)
www.zju.edu.cn/jzus; www.springerlink.com
E-mail: jzus@zju.edu.cn

Elastoplastic pipe-soil interaction analyses of partially-supported jointed water mains*

Yu SHAO†, Tu-qiao ZHANG

(*Department of Civil Engineering, Zhejiang University, Hangzhou 310027, China*)

†E-mail: shaoyu1979@zju.edu.cn

Received June 21, 2007; revision accepted Oct. 21, 2007; published online Jan. 17, 2008

Abstract: Water distribution networks are essential components of water supply systems. The combination of pipe structural deterioration and mechanics leads to the failure of pipelines. A physical model for estimating the pipe failure must include both the pipe deterioration model and mechanics model. Winkler pipe-soil interaction (WPSI), an analytical mechanics model developed by Rajani and Tesfamariam (2004), takes external and internal loads, temperature changes, loss of bedding support, and the elastoplastic effect of soil into consideration. Based on the WPSI model, a method to evaluate the elastic and plastic areas was proposed in the present study. An FEM model based on pipe-soil interaction (PSI) element was used to verify the analytical model. Sensitivity analyses indicate that the soft soil, long pipe and high temperature induced the axial plastic deformation more likely, which, however, may not occur in normal scenarios. The soft soil, pipes in small diameters, long unsupported bedding are prone to form flexural plastic area. The results show that the pipes subjected to the same loads have smaller stresses in the elastoplastic analysis than elastic analysis. The difference, however, is slight.

Key words: Elastoplastic soil, Winkler pipe-soil interaction (WPSI), Jointed water mains
doi:10.1631/jzus.A071327 **Document code:** A **CLC number:** TU435

INTRODUCTION

Buried water mains are designed to withstand certain design loads including soil load, truck/live load, working pressure, and water hammer pressure. The pipe material and wall thickness are chosen to withstand these loads. Pipes located in regions prone to freezing temperatures, sometimes experience an additional load caused by frost heaving of surrounding soil and the expansion of the soil (Zhan and Rajani, 1997). Similarly, wide and rapid temperature variations in the soil environment and pipes lead to additional thermal stresses in the pipe. Leakage in pipes and bad construction practices around pipes lead to pipe bed disruption.

It is a generally accepted notion that small diameter mains (150~200 mm) are susceptible to circumferential ruptures, whereas larger diameter pipes (≥250 mm) are prone to longitudinal breaks (O'Day *et al*., 1986). Longitudinal breaks are attributed to ring failure or crushing, whereas circular breaks are considered to be caused by beam failure due to a longitudinal tensile stress. Studies of water main break histories indicate that a drop in seasonal temperatures is almost always followed by an increase in the number of breaks, and that the frequency of break rate increases with a decrease in pipe diameter (Rajani *et al.*, 1996). The failure statistics for cities in China are not available in literature, and the information of pipe failure is still scattered within water supply companies. Table 1 is statistics about the total pipe lengths, pipe material proportions, and leak rates for three cities and one province in China in 2004.

To deal with the small diameter pipe failures due to temperature difference and bed disruption, the Winkler pipe-soil interaction (WPSI) model

* Project supported by the National Natural Science Foundation of China (No. 50278088) and the Program for New Century Excellent Talents in University (No. NCET-04-0525), China

Table 1 Statistics of pipe materials and leak rates (CWSA, 2004)

Cities and Province	D>75 mm pipe length (km)	Distribution density (km/km^2)	Pipe materials						Leak rate (%)
			Ductile iron (%)	Steel (%)	Cast iron (%)	Concrete (%)	Plastic (%)	Other (%)	
Beijing	6307.7	11.81	−	29.59	66.05	2.36	0.73	1.27	15.94
Shanghai	14191.1	9.53	16.04	3.63	35.46	3.85	34.92	6.09	18.67
Tianjin	5146.0	9.56	24.09	4.64	41.86	0.53	17.98	10.91	14.35
Zhejiang	15148.5	4.70	26.20	11.30	27.23	20.32	6.21	8.73	16.57

developed by Rajani and Tesfamariam (2004) has the following assumptions:

(1) The analyses of axial and flexural responses of buried jointed pipe are uncoupled;

(2) The pipe deformations are small and always within the elastic range;

(3) The elastoplastic Winkler soil model is used to model the soil resistance;

(4) The unsupported bedding is located in the center of the pipe, which represents the worst-case scenario;

(5) The pipe end is jointed and free in small axial movement and slight rotation. We can consider there are no axial stress and movement at the pipe end.

Although in general the Winkler model has several shortcomings, it is considered as "an acceptably simple model to permit the consideration of axial effects, longitudinal bending and radial effects associated with overburden pressures, internal pressure, frost loads, and thermal effects" (Rajani and Tesfamariam, 2004). This physical deterministic model for pipe-soil interaction (PSI) provides fixed values in determining safety factors. To consider the uncertainty, Sadiq *et al.*(2004) used Monte Carlo simulations to estimate the probability of pipe failures at a given time, and Tesfamariam *et al.*(2006) utilized the fuzzy-based possibility approach to predict the corrosion-associated failures in cast iron water mains, where the basic physical model was WPSI model.

However, the method to calculate the elastic area and plastic area was not considered in (Rajani and Tesfamariam, 2004). We found that the axial stress by elastoplastic analysis was larger than that by elastic analysis in (Rajani and Tesfamariam, 2004). The same result can be applied to the flexural stress. However, this phenomenon conflicts with common sense. The elastoplastic soil has little resistance compared to the elastic soil when deformation exceeds the elastic limit. Therefore, elastoplastic soil offers smaller resistance than elastic soil, and thus the stresses induced by elastoplastic soil should be lower than those induced by elastic soil. We postulate that this unreasonable result may be due to a subjective assumption of elastic area and plastic area, rather than an actual evaluation.

In Section 2, we briefly recall the governing equations and boundary conditions of the axial and flexural PSI model of Rajani and Tesfamariam (2004), then propose a method of calculating the elastic area and plastic area. In Section 3, we performed the sensitive analysis of the parametric study that affects the plastic behavior of soil. Then, the comparison between the elastoplastic results and elastic results was given. In Section 4, the FEM model based on PSI element (ABAQUS, 2002) using the same parameters of the analytical WPSI model is applied to validate the analytical result. The numerical result agrees with the analytical result very well, which indicates that the first assumption may be reasonable. Finally, some conclusions were given in Section 5.

GOVERNING EQUATIONS AND BOUNDARY CONDITIONS

External and internal loads and temperature changes cause various stresses on the pipe wall, including ring, hoop, longitudinal, and flexural (bending) stresses as shown in Fig.1. We focus on the method for calculating the longitudinal stress σ_x^{a} and flexural stress σ_x^{f}.

Axial elastoplastic PSI

Soil has been assumed as an elastoplastic material (Fig.2a). If the axial deformation exceeds the limiting axial displacement, the problem should be solved piecewise in three regions, i.e., the

unsupported area (*b*), the elastic area (*d*), and the plastic area (*f*) (Fig.2b). Rajani and Tesfamariam (2004) proposed the basic Eq.(1) to solve the axial PSI.

The piecewise governing equations are:

$$\begin{cases} \dfrac{\partial \sigma_x^{\mathrm{a}}}{\partial x} = 0 & \text{(unsuported area);} \\ \dfrac{\partial \sigma_x^{\mathrm{a}}}{\partial x} - \dfrac{k_{\mathrm{s}}^{\mathrm{a}}}{t} u_{\mathrm{d}} = 0 & \text{(elastic area);} \\ \dfrac{\partial \sigma_x^{\mathrm{a}}}{\partial x} - \dfrac{F_x}{t} = 0 & \text{(plastic area).} \end{cases} \tag{1}$$

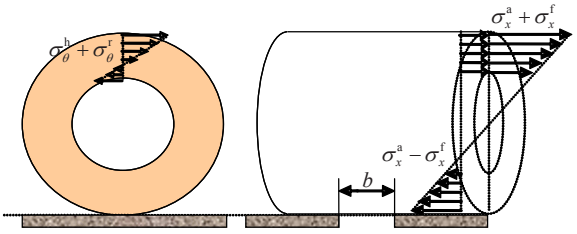

Fig.1 The stress of the buried pipe

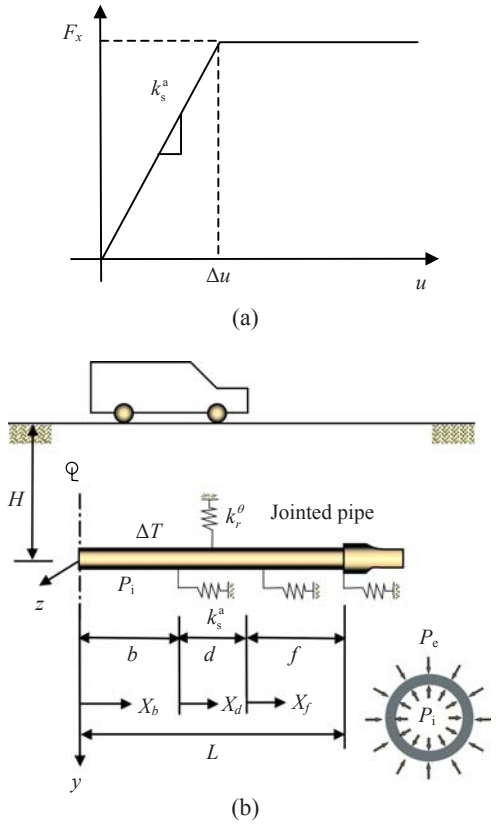

Fig.2 (a) Axial soil resistance versus axial displacement; (b) Schematic model for axial pipe-soil interaction (Rajani and Tesfamariam, 2004)

The axial stress σ_x^{a} has the following form:

$$\sigma_x^{\mathrm{a}} = \chi_1 E_{\mathrm{p}} \frac{\partial u}{\partial x} + \chi_2 P_{\mathrm{i}} - \chi_3 E_{\mathrm{p}} \alpha_{\mathrm{p}} \Delta T, \tag{2}$$

where, χ_1, χ_2, χ_3 defined by Rajani *et al*.(1996) are constants.

Substituting Eq.(2) for σ_x^{a} in Eq.(1), by assuming that the internal pressure P_{i} and temperature difference ΔT do not change along the pipe, we get the differential equation expressed by axial displacement u. By solving it, the general solutions are:

$$\begin{cases} u_b = B_1^{\mathrm{a}} x_b + \alpha_{\mathrm{p}} \Delta T x_b + B_2^{\mathrm{a}} & \text{(unsuported area);} \\ u_d = C_1^{\mathrm{a}} \mathrm{e}^{(-\gamma x_d)} + C_2^{\mathrm{a}} \mathrm{e}^{(+\gamma x_d)} & \text{(elastic area);} \\ u_f = \dfrac{F_x}{2tE_{\mathrm{p}}\chi_1} x_f^2 + F_1^{\mathrm{a}} x_f + \alpha_{\mathrm{p}} \Delta T x_f + F_2^{\mathrm{a}} & \text{(plastic area),} \end{cases} \tag{3}$$

where, the 6 coefficients B_1^{a}, B_2^{a}, C_1^{a}, C_2^{a}, F_1^{a}, F_2^{a} should be solved by the following boundary equations:

$$\begin{cases} u_b(x_b = 0) = 0, \\ u_b(x_b = b) = u_d(x_d = 0), \\ u_b'(x_b = b) = u_d'(x_d = 0), \\ u_d(x_d = d) = u_f(x_f = 0), \\ u_d'(x_d = d) = u_f'(x_f = 0), \\ \sigma_x(x_f = f) = 0. \end{cases} \tag{4}$$

The coefficients can be easily solved by software such as Maple and Mathematica. Since the analytical solution of axial displacement u is attained, by substituting Eq.(3) for $\partial u/\partial x$ in Eq.(2), we get the stress solution.

Determination of *d* and *f* for axial PSI

Actually, if the load ΔT is small and the soil axial resistance is large, the pipe axial displacement does not reach the limiting axial displacement Δu, and the plastic area may not be formed. By comparing $u_d(x_d=L-b)$ with Δu, we can judge whether the soil has the plastic area.

If

$$u_d(x_d=L-b) \le \Delta u, \tag{5}$$

there must be no plastic area. And we should set f=0. The solutions degrade to elastic solution.

If

$$u_d(x_d=L-b)>\Delta u,\quad u_d(x_d=b)\le\Delta u, \tag{6}$$

we can conclude that the soil has plastic and elastic areas. The state transformation point between the plastic and elastic areas can be obtained by solving

$$\begin{cases} u_f(x_f=0)=\Delta u \quad \text{or} \quad u_d(x_d=d)=\Delta u, \\ d+f=L-b, \end{cases} \tag{7}$$

where d and f are variables that should be solved. However, Eq.(7) includes cosh(dγ) and sinh(dγ) items. The variables d and f cannot be solved analytically. We use the mathematical software Maple to solve the variables d and f numerically. The command is as follows:

f:=fsolve(subs(d=L−b−f, u_f(0)−Δu), f=0..L−b).

Flexural elastoplastic PSI

Similarly, the soil is assumed as an elastoplastic material. If the flexural deformation exceeds the limiting flexural displacement, the problem should be solved piecewise in three regions, i.e. unsupported area (b), plastic area (c), and elastic area (e) (Fig.3). We assumed that the pipe settlements are uniform considering the act of the soil weights loads, until the bed disruption occurs. The unsupported bedding results in the flexural deformation of pipes, which leads to flexural stress. Rajani and Tesfamariam (2004) gave the basic Eq.(8) and Eq.(10) to solve the flexural PSI.

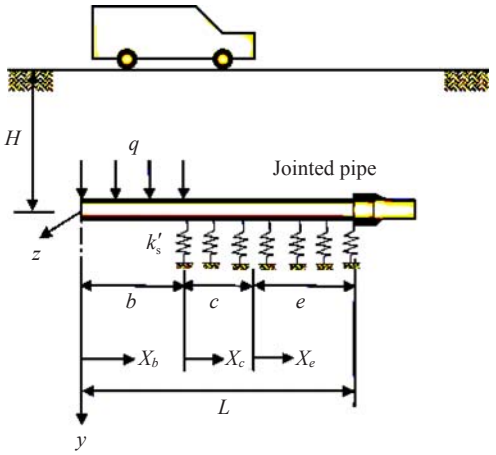

Fig.3 Schematic model for flexural pipe-soil interaction (Rajani and Tesfamariam, 2004)

The piecewise governing equations are:

$$\begin{cases} E_{\mathrm{p}}I_{zz}\dfrac{\partial^4 v_b}{\partial x^4}=q \quad \text{(unsuported area)}, \\ E_{\mathrm{p}}I_{zz}\dfrac{\partial^4 v_c}{\partial x^4}+F_y=0 \quad \text{(plastic area)}, \\ E_{\mathrm{p}}I_{zz}\dfrac{\partial^4 v_e}{\partial x^4}+k'_{\mathrm{s}}v_e=0 \quad \text{(elastic area)}. \end{cases} \tag{8}$$

By solving the differential Eq.(8), the general solutions are:

$$\begin{cases} v_b=\dfrac{qx_b^4}{24E_{\mathrm{p}}I_{zz}}+\dfrac{B_1x_b^3}{6}+\dfrac{B_2x_b^2}{2}+B_3x_b+B_4, \\ v_c=\dfrac{-F_yx_c^4}{24E_{\mathrm{p}}I_{zz}}+\dfrac{C_1x_c^3}{6}+\dfrac{C_2x_c^2}{2}+C_3x_c+C_4, \\ v_e=\mathrm{e}^{\lambda x_e}[E_1\cos(\lambda x_e)+E_2\sin(\lambda x_e)]+ \\ \qquad \mathrm{e}^{-\lambda x_e}[E_3\cos(\lambda x_e)+E_4\sin(\lambda x_e)], \end{cases} \tag{9}$$

where, the 12 coefficients B_1~B_4, C_1~C_4, E_1~E_4 should be solved by using boundary conditions. Assume that the pipe end has no vertical displacement and no moment, i.e., $v_e(x_e=e)=0$, $v''_e(x_e=e)=0$. Considering the symmetry in the center of a pipe, we have zero rotation $v'_b(x_b=0)=0$ and zero shear $v'''_b(x_b=0)=0$. By using the continuity and compatibility at $x_b=b$ and $x_c=0$, the displacement v, and its first- to third-order derivative should be equal. At $x_c=c$ and $x_e=0$, we have similar boundary conditions. Together we have 12 boundary conditions, and the 12 coefficients can be solved. Then the vertical displacement solution is obtained.

According to the relations between the rotation, moment, shear and displacement, we have

$$\begin{cases} \theta=\tan^{-1}(v'), \\ M_x=-E_{\mathrm{p}}I_{zz}v'', \\ Q=-E_{\mathrm{p}}I_{zz}v'''. \end{cases} \tag{10}$$

The maximum flexural stress in the pipe wall can be expressed as $\sigma_x^{\mathrm{f}}=M_xR/I_{zz}$.

Determination of *c* and *e* for flexural PSI

Similarly, if the load q is small and the soil axial resistance is large, the pipe vertical displacement does not reach the limiting vertical displacement Δv, and the plastic area may not be formed. By comparing $v_e(x_e=0)$ with limiting vertical displacement Δv, we can judge whether the soil have the plastic area.

If

$$v_e(x_e=0)\leq\Delta v, \tag{11}$$

there must be no plastic area. And we should set c=0. The solutions degrade to elastic solution.

If

$$v_e(x_e=0)\geq\Delta v,\ \ v_e(x_e=L-b)\leq\Delta v, \tag{12}$$

we can conclude that the soil has plastic area and elastic area. The state transformation point between plastic and elastic areas can be obtained by solving

$$\begin{cases} v_c(x_c=c)=\Delta v \ \text{ or } \ v_e(x_e=0)=\Delta v, \\ c+e=L-b, \end{cases} \tag{13}$$

where c and e are variables that should be solved. However, Eq.(13) has $e^{(\lambda x_e)}$ and $\tan(\lambda x_e)$ items, so we must solve c and e numerically. The mathematical software Maple is used to solve c and e by applying the command as:

c:=fsolve(subs($e=L-b-c$, $v_e(0)-\Delta v$), c=0..$L-b$).

SENSITIVE ANALYSIS

Axial plastic area

A sensitive analysis was carried out to investigate whether the soil can have a plastic area to different pipe lengths, soil stiffness, temperature changes, and pipe materials. Three 150 mm pipes made of DI, CI, or PVC in medium sand with k_s^a being 125 MPa/m were selected as references. The soil and material properties in the references were chosen from Table 1. Every time we let one of parameters change to gauge its sensitivity of the PSI (Figs.4a and 4b).

As previously mentioned, if $u_d(x_d=L-b)>\Delta u$, we can infer that the soil yields. The elastic axial maximum displacement (Fig.4a) decreased as the soil axial modulus increased, since the stiffer soil could give more resistance to constrain the pipe movement. The soil modulus had less influence on CI and DI pipes than on PVC pipe due to the ratio between the pipe elastic modulus and soil elastic modulus. We can find that only the PVC pipe could reach the limiting axial displacement Δu=2.5~5.0 mm, as the guidelines (CGLFL, 1984) suggested when the soil was very soft (Fig.4a). For CI and DI pipes, the axial maximum displacement without considering the soil resistance can be calculated as

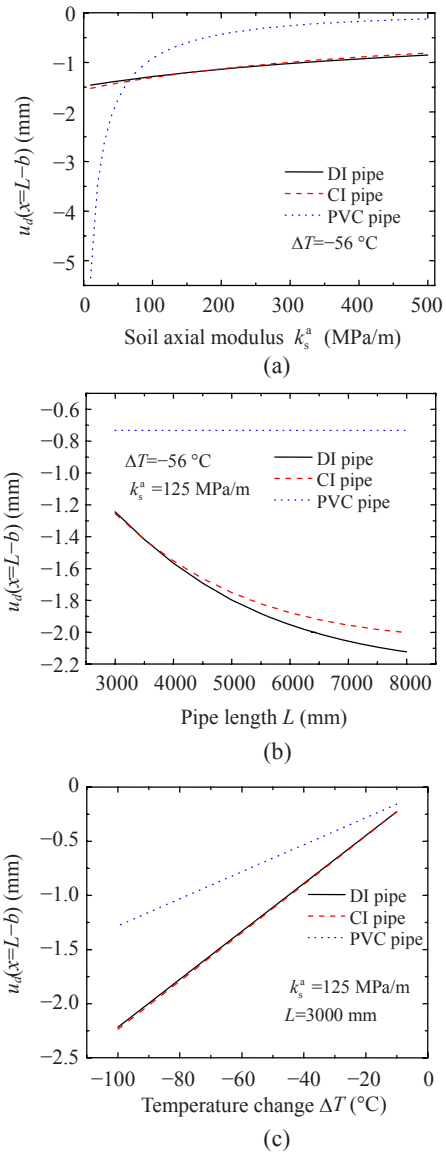

Fig.4 The effect of (a) soil axial modulus, (b) pipe length and (c) temperature change on elastic maximum displacement

$$u=\alpha\Delta TL=1.05\times10^{-5}\times56\times3000=1.764,$$

which is smaller than Δu.

Fig.4b shows the effect of pipe lengths. Because of the small elastic modulus of PVC pipe, the length had no influence on its elastic axial maximum displacement, while the axial displacement of the CI and DI pipes increased as the pipe length increased. However, the displacement of DI pipe had only 2.1 mm, until the length L reaches 8 m.

Fig.4c shows the effect of the temperature change on the elastic maximum displacement. As temperature change increased, the axial displacement increased, too.

The sensitivity analysis indicates that the soft soil, long pipe and large temperate change were prone to form the plastic area. The soil axial modulus had greater influence on PVC pipes, while the pipe length and temperature change gave more significant effects on DI and CI pipes.

Flexural plastic area

Similarly, we took a sensitive analysis to investigate a flexural plastic area against different pipe diameters, soil stiffness, external loads, unsupported bedding length, and pipe materials. Three 150 mm pipes made of DI, CI, or PVC material were selected as references. The material parameters were taken from Table 1.

As previously mentioned, if $v_e(x_e=0)\geq\Delta v$, we can infer that the soil yields. The elastic vertical maximum displacement (Fig.5a) decreased as the soil flexural modulus increased. And the PVC pipe was prone to yield easily due to its small elastic modulus. Fig.5b indicates that small diameter pipe had larger displacement than large diameter pipe because of lower second moment of inertia. The small diameter pipes had more chances to yield for the limiting displacement, which is relevant to the pipe. The guidelines (ALA, 2001) suggest that the limiting displacement is 0.1D for granular soils and 0.2D for cohesive soils.

Since stiffer soil modulus hardly leads to soil yield, lower soil flexural modulus such as 5 MPa was chosen to investigate the effect of unsupported bedding length and external loads on soil plastic behavior.

The elastic vertical maximum displacement

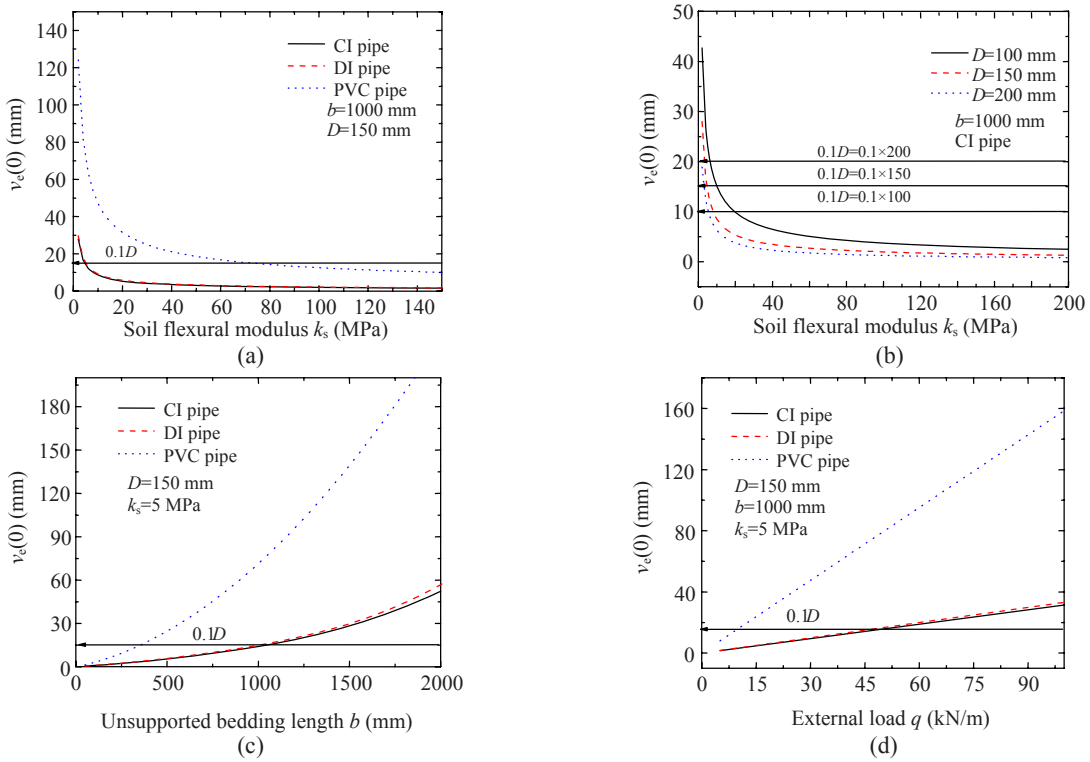

Fig.5 The effect of (a) soil flexural modulus, (b) pipe diameter, (c) unsupported bedding length and (d) external loads on elastic maximum vertical displacement

(Fig.5c) increased as the unsupported bedding length increased. The PVC pipe first began to yield when the unsupported bedding length was less than 500 mm, while the DI and CI pipes needed the unsupported bedding length to be more than 1000 mm. Similar situations can be found for the effect of the external loads (Fig.5d).

The sensitive analysis indicates that the soft soil, small diameter pipe, bad supporting bedding and large external loads were prone to form the vertical plastic area.

Comparison between elastoplastic and elastic analysis

As previously mentioned, long pipe and large temperature change could cause the soil to yield. Therefore, we set the temperature difference as −56 °C and pipe length as 4 m. The elastoplastic response of the soil was artificially induced in this example by decreasing the limiting axial displacement as −1.5 mm. The elastoplastic and elastic responses of pipes with an unsupported length of b=500 mm were shown in Fig.6a. The plastic area length measured 658.4 mm. The consideration of elastoplastic of soil decreases the axial stresses induced in the pipe compared with elastic analysis only, as the soil of elastic model was stiffer than that of elastoplastic model if the soil began to yield, and could offer more resistance. However, the difference between the elastoplastic and elastic analyses was small. We could obtain conservative results if we substitute the elastic model for the elastoplastic model.

Similar results and conclusion came from the elastoplastic analysis of flexural bending. We set the flexural modulus to be 5 MPa, external loads 60 kN/m, and limiting vertical displacement 0.1D. Fig.6b shows that the result of elastoplastic analysis was slightly smaller than that of elastic analysis.

Figs.6a and 6b show lower axial stress and flexural stress responses induced by the elastoplastic analysis than those induced by the linear elastic analysis. The results differ from those of Rajani and Tesfamariam (2004), who obtained a larger stress response in the elastoplastic analysis. The elastoplastic soil has no additional resistance as the axial displacement reaches the elastic limit Δu, while the linear elastic soil will offer more resistance when larger axial displacement occurs. So the elastoplastic soil

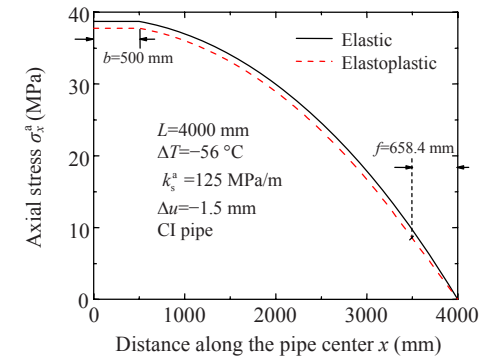

Fig.6 Comparison of the elastic and elastoplasitc analyses for axial stress (a) and for flexural stress (b)

has less resistance than elastic soil when the axial deformation exceeds the elastic limit. The jointed water main is assumed to be moved freely in the joint. The only resistance against pipe axial moving is the soil axial friction. Given a limiting example that if the soil is so soft that k_s^a =0, the pipe can move in the axial direction freely and has no axial stress. Since the elastoplastic soil offers smaller resistance than the elastic soil does, the stress induced by the elastoplastic soil should be lower than that induced by the elastic soil, if other conditions are identical. The method to calculate the elastic length d and plastic length f for axial PSI, as well as c and e for flexural PSI could not be found in Rajani and Tesfamariam (2004)'s study. However, they gave d=485 mm, resulting in different results. We guess that the plastic area was assumed subjectively by Rajani and Tesfamariam (2004), rather than evaluated by practical considerations. Actually, substituting their model parameters into Eqs.(5)~(7) to calculate the plastic and elastic areas, we found that the real plastic area was zero. Therefore, we set the plastic area at 485

mm, and obtained the same result as Rajani and Tesfamariam (2004)'s. Obviously, this is unreasonable, because the real plastic area is zero, not 485 mm. The FEM model will be used to validate the analytical results in Section 4. The FEM simulation result supports the analytical result very well, indicating that the results of elastoplastic analysis of Rajani and Tesfamariam (2004) was questionable. In short, solving Eq.(7) or Eq.(13) to determine the plastic area and elastic area is the most important step for elastoplastic analysis.

FEM SIMULATION USING PSI ELEMENT

ABAQUS provides a library of PSI elements to model the interaction between a buried pipeline and the surrounding soil. The pipeline itself was modeled with any of the beam and pipe elements. The soil-pipe interaction was modeled with the PSI elements. These elements only have displacement degrees of freedom at their nodes. One side or edge of the element shares nodes with the underlying pipe element that models the pipeline. The nodes on the other edge represent a far-field surface. The pipe-soil stiffness could constitute the linear elastic constitutive model, nonlinear constitutive model, and ASCE model. The nonlinear constitutive model and ASCE model could consider the axial, lateral, uplift and downward stiffness.

Here we used the nonlinear constitutive model to validate the analytical WPSI model. A half of model was meshed for analysis because of the model symmetry. The half model had 50 pipe elements (20 in the unsupported area and 30 in the supported area) and 50 PSI elements (Fig.7). The same pipe and soil parameters, loads and boundary conditions as ones used in the previous WPSI model were chosen. However, the definition of the axial elastic modulus of the FEM was different from the previous analytical WPSI model. The axial modulus $k_s^{a\prime}$ used in ABAQUS should be $k_s^a \pi D$, where k_s^a was used in analytical WPSI model, and D was the pipe outside diameter. The loads such as the pipe internal pressure, overburden load, and temperature change were applied on the pipe. The magnitude of the loads was the same as the previous analytical WPSI model. The soil far-field boundary was fixed and the symmetry boundary was adopted in the center of the pipe. The 20 PSI elements in the unsupported area should be killed to simulate the lost soil after the analysis started.

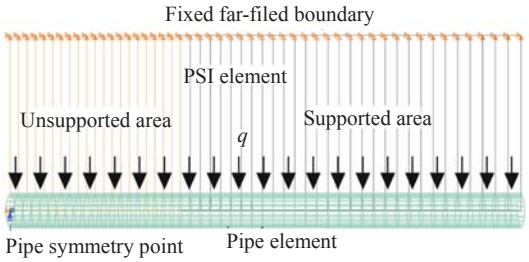

Fig.7 Pipe-soil model mesh and boundary

Setting ΔT as zero, we considered stress induced by the pipe flexural bending only. The result was compared with the analytical solution as shown in Fig.8a. The results show that the numerical solution agreed well with the analytical one. Their curves were overlapped completely.

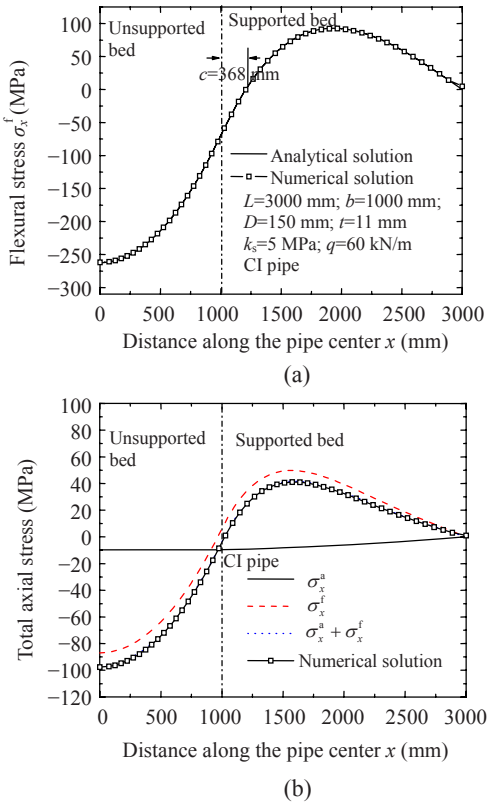

Fig.8 Analytical and numerical solutions for flexural stress (a) and for total axial stress (b)

Adding temperature change ΔT, external loads q and the internal pressure P_i into the FEM model, we got the stress of the pipe in the below point of pipe section, which agreed well with the sum of analytical

axial stress σ_x^a and flexural stress σ_x^f. The curves of numerical solution and $\sigma_x^a+\sigma_x^f$ as shown in Fig.8b were overlapped, suggesting that the uncoupled axial and flexural analysis for small deformation of pipe was suitable.

Cast iron material has different material properties in tension and compression. However, we still use the linear elastic material model in the analytical WPSI model for simplicity. If the nonlinear cast iron material model is used, the relation of moment and the pipe curvature is very complicated, i.e., Eq.(8) will not be held. There still needs further work to obtain an analytical solution for nonlinear material model.

However, using the FEM simulation, the nonlinear material model of cast iron material can easily be applied. The cast iron material property was chosen from Coffin (1950)'s experimental data (Fig.9). The moment and flexural stress of the linear elastic pipe material and cast iron pipe material were compared. In the first case, a flexural soil modulus k_s=50 MPa and an overburden load q=60 kN/m were chosen to simulate. However, the difference of the moment and stress with two different materials was not obvious (Fig.10), as the pipe was almost working in the elastic stage under such loading condition. In the second case, a larger load q=100 kN/m, and a softer soil k_s=5 MPa were chosen. The moment and stress with cast iron material were more reasonable than those with linear elastic material as shown in Fig.11.

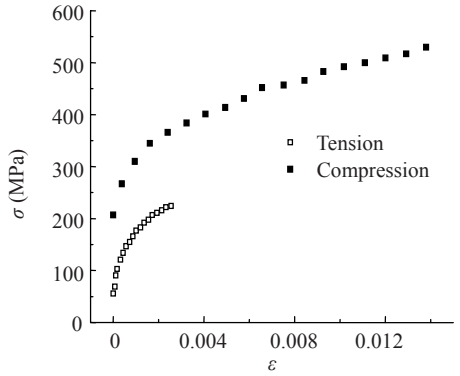

Fig.9 Cast iron material property

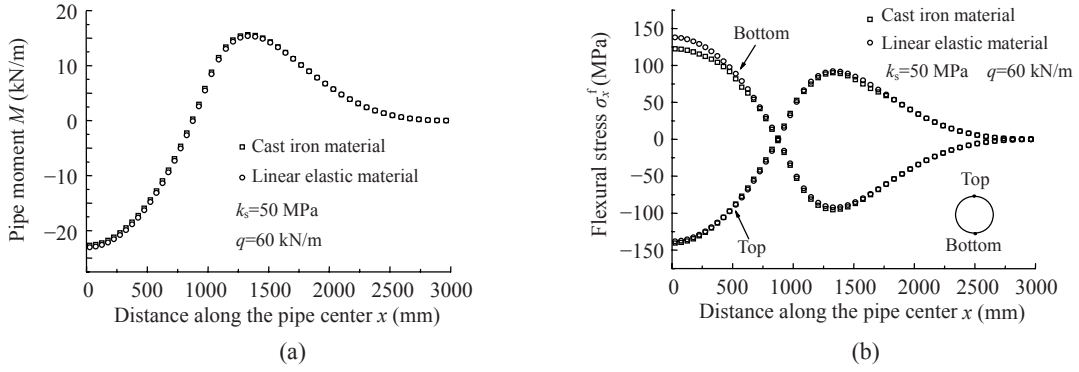

Fig.10 Comparison of the moment (a) and flexural stress (b) with k_s=50 MPa and q=60 kN/m

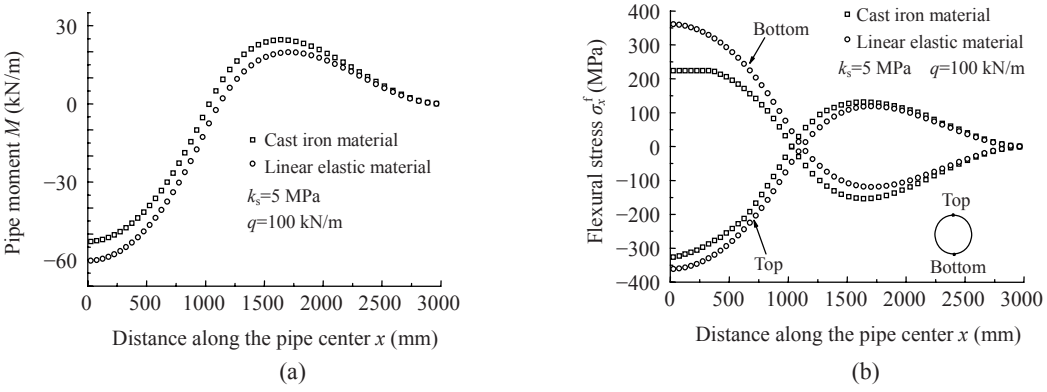

Fig.11 Comparison of the moment (a) and flexural stress (b) with k_s=5 MPa and q=100 kN/m

CONCLUSION

Based on the WPSI model, we offered a method to evaluate the elastic and plastic areas. An FEM model based on PSI element is used to verify the analytical model. The conclusions of the present paper are summarized as follows:

The soft soil, long pipe and large temperature change are prone to form the axial plastic area. The soil axial modulus has more influence on the PVC pipe, while the pipe length and temperature change give significant effect on the DI and CI pipes. The soft soil, small diameter pipes, poor bedding support and large external loads are prone to form the vertical plastic area. However, in normal environment, the possibility of forming plastic area is small for both axial and vertical plastic areas.

Both axial and flexural stresses of elastoplastic analysis are slightly smaller than those of elastic analysis. Using the elastic analytical results to substitute for the elastoplastic analysis is conservative.

The FEM simulation results agreed well with the results of the analytical WPSI model, which suggests that the uncoupled axial and flexural PSI analysis is reasonable for a small deformation of a pipe.

References

ABAQUS, 2002. ABAQUS/Standard User's Manual; ABAQUS/CAE User's Manual; ABAQUS Keywords Manual. HKS Inc., America.

ALA (American Lifelines Alliance), 2001. Guideline for the Design of Buried Steel Pipe. Http://www.amercanlifelinesalliance.org

CGLFL (Committee on Gas and Liquid Fuel Lifelines), 1984. Guidelines for the Seismic Design of Oil and Gas Pipeline Systems. America Society of Civil Engineering, New York.

Coffin, L.F., 1950. The flow and fracture of a brittle material. *Journal of Applied Mechanics*, **72**:233-248.

CWSA (China Water Supply Association), 2004. Statistical Yearbook on Water Supply of Chinese Cities. The State Statistical Bureau, Beijing (in Chinese).

O'Day, D.K., Weiss, R., Chiavari, S., Blair, D., 1986. Water Main Evaluation for Rehabilitation/Replacement. AWWARF and AWWA, Denver, Colo.

Rajani, B., Tesfamariam, S., 2004. Uncoupled axial, flexural, and circumferential pope-soil interaction analyses of partially supported jointed water mains. *Canadian Geotechnical Journal*, **41**(6):997-1010. [doi:10.1139/t04-048]

Rajani, B., Zhan, C., Kuraoka, S., 1996. Pipe-soil interaction analysis for jointed water mains. *Canadian Geotechnical Journal*, **33**(3):393-404.

Sadiq, R., Rajani, B., Kleiner, Y., 2004. Probabilistic risk analysis of corrosion associated failures in cast iron water mains. *Reliability Engineering & System Safety*, **86**(1):1-10. [doi:10.1016/j.ress.2003.12.007]

Tesfamariam, S., Rajani, B., Sadiq, R., 2006. Possibilistic approach for consideration of uncertainties to estimate structural capacity of ageing cast iron water mains. *Canadian Journal of Civil Engineering*, **33**(8):1050-1064. [doi:10.1139/L06-042]

Zhan, C., Rajani, B., 1997. On the estimation of frost load in a trench: theory and experiment. *Canadian Geotechnical Journal*, **34**(4):568-579. [doi:10.1139/cgj-34-4-568]